

Design of Compact Dual Circularly Polarized Ring Series-Fed Quasi-Lumped Antenna Array

Yazeed Qasaymeh^{1, *}, Abdullah Almuhasien¹, and Khaled Issa²

Abstract—A differentially compact dual circularly polarized (CP) ring traveling wave-fed quasi-lumped resonator (QLR) array working at 5.8 GHz is presented. The array consists of seven series QLRs, each with an interdigital finger capacitor, connected by a parallel narrow-strip inductor. The CP was obtained by organizing the radiating QLR over a series ring-fed microstrip. The QLR was fed with a current of the same magnitude and some phase delay at each element. The dual-port feeding permitted the selection of the traveling wave direction and, consequently, the mode of CP. The measured bandwidth was 5.76–5.8 GHz at port 1. Meanwhile, the bandwidth was 5.75–5.77 GHz at port 2. The measured peak gain was 5.9 dBi at port 1 and 6.4 dBi at port 2. The cross-polarization was 19 dB lower than the co-polarization at port 1, which is a characteristic of right-hand circular polarization (RHCP). The cross-polarization was 14 dB higher than the co-polarization at port 2, which is a characteristic of left-hand circular polarization (LHCP). The size of each radiating element was $5.8 \times 5.6 \text{ mm}^2$, and the array was $40 \times 40 \text{ mm}^2$. These features and its compact size make the proposed array antenna a good candidate to be used in wireless systems.

1. INTRODUCTION

A dual circularly polarized (CP) antenna is an essential component in fully polarized systems, including, but not limited to, radar, navigation, and wireless communication [1]. Compared to a conventional CP antenna, the dual-CP antenna increases the wireless communication capacity owing to its attractive feature of combating the multipath fading effect [2, 3]. Consequently, studies on augmenting the functionalities of the dual-CP antenna and realizing them have become trending [4].

Many dual-CP antennas have been studied in the open literature and can be classified into two main divisions: cross-dipole antennas [5, 6] and patch antennas [7, 8]. Lately, various dual-CP patch antenna arrays have been presented. The latter can be categorized into two main types: serially fed [9–11] and parallel fed ones [12, 13]. Moreover, dual-CP patch antennas can also be categorized into differentially fed antennas [14] and commonly fed antennas [15]. Differential circuits are more convenient to integrate with differentially fed antennas [16]. Most of the reported multiport dual-CP antennas are differentially fed [15]. Various differentially fed dual-CP antennas have been documented in the literature. A cavity-backed patch differentially fed dual-CP antenna was reported in [17]. An ultra-wideband differentially fed dual-CP antenna was presented in [18]. A dual-CP differentially fed antenna with a magnetoelectric structure was reported in [19]. A dual-CP differentially fed multidipole antenna was documented in [20].

A few rounded dual-CP antenna arrays have been reported in the literature. Luo and Chu (2016) presented a parallel sequentially rotated dual-CP array with a complex structure [21]. A Wilkinson power-divider dual-CP microstrip patch array was reported in [12]. A series traveling wave circular

Received 22 December 2019, Accepted 10 June 2020, Scheduled 23 June 2020

* Corresponding author: Yazeed Qasaymeh (y.qasaymeh@mu.edu.sa).

¹Department of Electrical Engineering, Faculty of Engineering, Majmaah University, 11952, Saudi Arabia. ²KACST-TIC in Radio Frequency and Photonics for the e-Society (RFTONICS), Electrical Engineering Department, King Saud University, Riyadh, Saudi Arabia.

microstrip-fed patch array was documented in [11]. Compared to parallel and sequentially fed arrangements, series-feed networks have the advantage of simplicity and compactness, which results into low-loss feeding structures.

In this communication, a compact seven-QLR element fed differentially by a series ring for a dual-CP antenna is presented. The proposed dual-CP antenna possesses right-hand circular polarization (RHCP) once it is excited from port one, and when it is fed from the second port, a left-hand circular polarization (LHCP) is obtained.

The paper is organized as follows. Section 2 discusses single-QLR geometry. The geometry of series-fed dual-CP arrays is presented in Section 3. Section 4 describes the theoretical analysis of power flow over series-fed arrays within uniform array elements. The experimental results and a discussion of the proposed antenna are presented in Section 5. Conclusions are drawn in Section 6.

2. SINGLE-ELEMENT ANTENNA CONFIGURATION

The quasi-lumped elements are much shorter than their own wavelengths. Thus, microstrips and stubs with physical extents are less than a quarter wavelength at a specified frequency and are components required for the estimated microwave operation of lumped elements in microstrip structures. Figure 1 shows a single quasi-lumped resonator. The planned resonator antenna is composed of a narrow straight strip inductor in parallel with an interdigital capacitor [22], whilst the equivalent lumped circuit is shown in Figure 2.

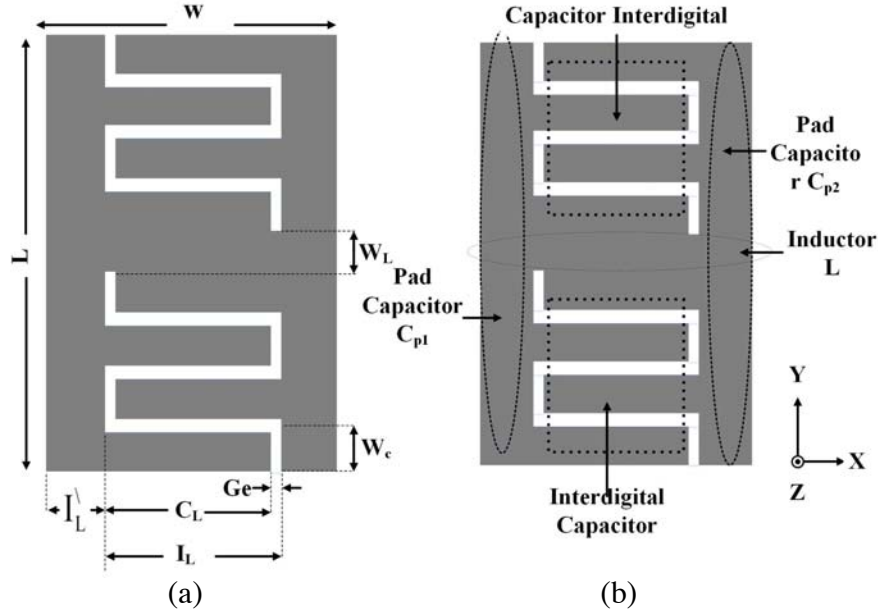


Figure 1. Proposed QLR: (a) dimensions used to calculate lumped elements, (b) allocation of lumped elements.

The equation to determine the resonant frequency of the proposed antenna is reported in [23–26]

$$f = \frac{1}{2\pi\sqrt{L\left(\frac{C_{p1}C_{p2}}{C_{p1} + C_{p2}} + C\right)}} \quad (1)$$

From Equation (1), the resonance frequency is confirmed by the equivalent lumped elements L , C_{p1} , C_{p2} , and C . These lumped elements are obtained by solving Equations (2) to (6) in an iterative manner using MATLAB®.

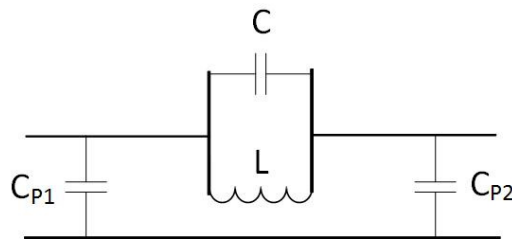


Figure 2. Equivalent circuit of proposed antenna.

The inductor L is a solo, thin, and straight conductor situated at the center. The inductance can be calculated by:

$$L = 200 \times 10^{-9} I_L \left(\ln \left(\frac{2I_L}{W_L + h} \right) + 0.50094 + \frac{W_L}{3I_L} \right) \quad (2)$$

where h is the substrate thickness.

The structure of interdigital capacitor C is a periodic multifinger. This capacitance occurs across a narrow slit between the conductors. These slits are very long. They are bent to minimize the area and, consequently, to minimize the used area attendant relevance as a lumped element. The structural series interdigitated capacitance is determined by:

$$C = \varepsilon_0 \left(\frac{\varepsilon_r + 1}{2} \right) (N - \Delta) C_L \quad (3)$$

where Δ is the correction factor $\Delta = 0.5(W_{eff} - w)$; W_{eff} is the effective width; w is the finger width; N is the fingers number.

The interdigital finger length of C_L is calculated by Equation (4). The width of the entire structure is calculated by Equation (5).

$$I_L = C_L + G_e \quad (4)$$

$$W = 2 \times I_L^{\perp} + I_L \quad (5)$$

The parasitic capacitors C_{P1} and C_{P2} at both ends of the structure act as capacitors to ground. By fine-tuning these capacitors, the resonant frequency of the resonator can be altered. The pad capacitance

Table 1. Quasi-lumped element parameters of proposed antenna.

Parameter	Dimension [mm]
w_e	0.35
I_L	3.35
C	3.05
N	8
I_L^{\perp}	1.23
g_e	1.23
W_L	1.2
L	5.4
W	5.8
h	0.813

values are determined using Equation (6):

$$C = \left(\frac{1}{25.4 \times 10^{-3}} \right) \times \left(\frac{2.8\epsilon_{eff}}{\ln \left(1 + \frac{1}{2} \left(\frac{8h}{\epsilon_{eff}} \right) \left(\frac{8h}{\epsilon_{eff}} + \sqrt{\frac{8h}{\epsilon_{eff}^2 + \pi^2}} \right) \right)} \right) \quad (6)$$

where h is the substrate height.

The physical dimensions of the radiating quasi-lumped element were derived from Equations (2) to (6). The dimensions of a single element at the aimed resonance of 5.8 GHz are listed in Table 1. The equivalent RLC lumped elements at the desired frequency are listed in Table 2. The dimensions and lumped elements were obtained by using Equations (2) to (6) at a resonant frequency of 5.8 GHz. The resonant frequency was calculated using Equation (1).

Table 2. Quasi-lumped element parameters of proposed antenna.

C	C_{p1}	C_{p2}	L
0.347 PF	0.17 PF	0.17 PF	1.47 nH

3. THE GEOMETRY OF SERIES-FED DUAL-CP ARRAYS

Figure 3 shows the proposed array of QLR. The configuration is described as seven QLR elements coupled to a concentric microstrip ring mounted on the top layer, differentially fed by two ports

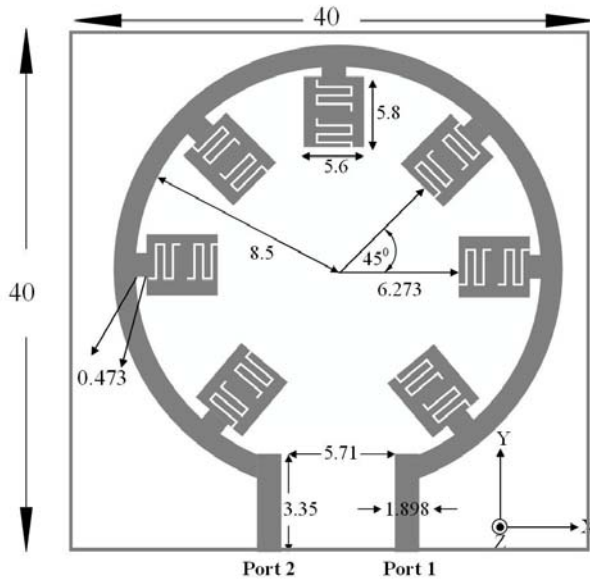


Figure 3. Configuration of proposed antenna [all spacings in mm].

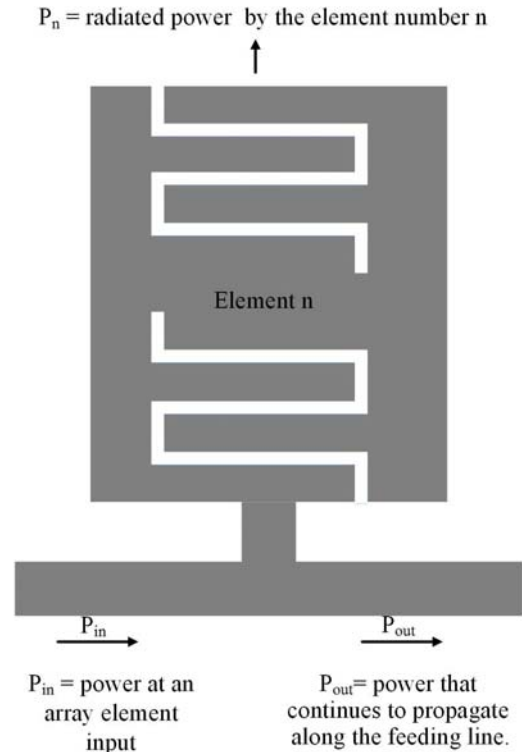


Figure 4. Power on single radiating element.

and grounded by the bottom layer. After being arranged in concentric ring, the QLRs are fed by phase-shifted current. These QLR elements resonate at a fundamental mode of circular polarization intrinsically generated by the travelling-wave excitation. The radiating elements are distributed evenly around the Z -axis. Thus, excitement of port 1 at a specified frequency results in RHCP, while LHCP is obtained by exciting port 2.

4. RADIATED POWER ANALYSIS OF ARRAY ELEMENTS

With a travelling-wave microstrip having a uniform series of array elements, the power is distributed to the radiating elements successively. Accordingly, power is successively fed to the radiation elements. If the power at an array element input is denoted as P_{in} , then P_n is the power radiated by that element, and P_{out} is the power that continues to propagate along the feeding line. Figure 4 describes the power flow geometry for a radiating element showing terms P_n , P_{in} , and P_{out} . The radiated power by each element can be determined by:

$$P = (1 - P_{n-1} - P_{n-2} - \dots - P_2 - P_1)\alpha = (1 - \alpha^{n-1})\alpha \quad (7)$$

where α is the power coupling coefficient, given by

$$\alpha = \frac{1 - |S_{11}|^2 - |S_{21}|^2}{1 - |S_{11}|^2} = \frac{P_n}{P_{in}} \quad (8)$$

where S_{11} is the reflection coefficient of each element, and S_{21} is the transmission coefficient of each element.

The total radiated power of an array of n elements is:

$$P_{\text{total}} = \sum_{n=1}^N P_N = 1 - (1 - \alpha^N) \quad (9)$$

where N is the number of array elements.

5. RESULTS AND DISCUSSION

The antenna prototype was fabricated on a Rogers substrate RO4003C with ϵ_r of 3.38 and thickness of 0.813 mm. This was experimentally characterized to validate the design. Figure 5 depicts the fabricated structures of the antenna with array of QLRs.

The seven-QLR device is progressively fed to radiate a portion of energy supplied by the guided wave traveling over the feedline from one port to the other. Nevertheless, the QLR is coupled with the same strength to the concentric feed, and it is expected that each QLR will radiate a decreasing

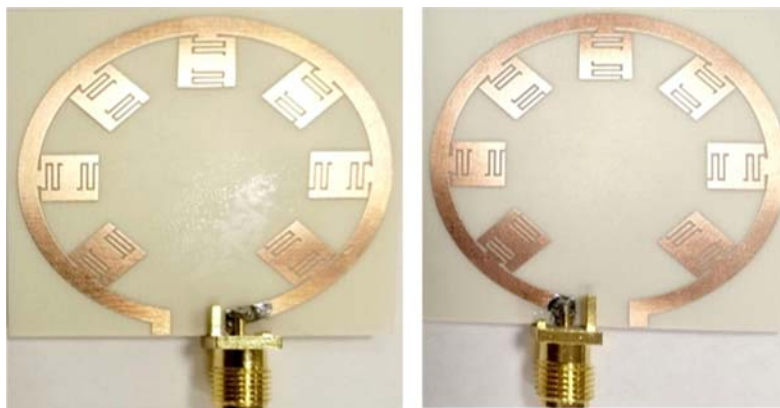


Figure 5. Front view of fabricated antenna, fed consecutively.

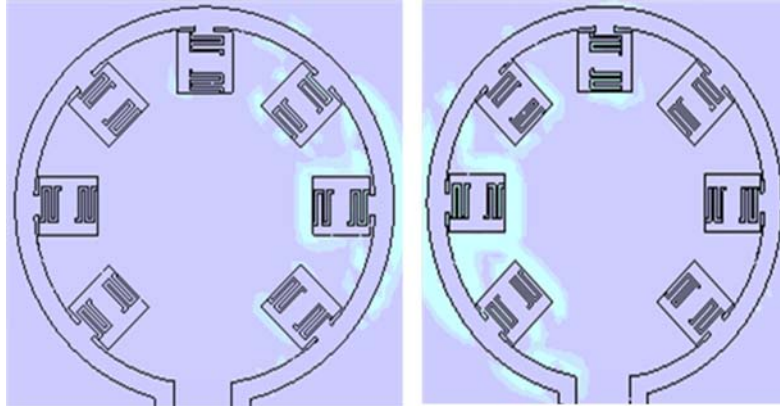


Figure 6. Radiated power strength over microstrip at 5.8 GHz from CST: (a) port 1 when port 2 is terminated, (b) port 2 when port 1 is terminated.

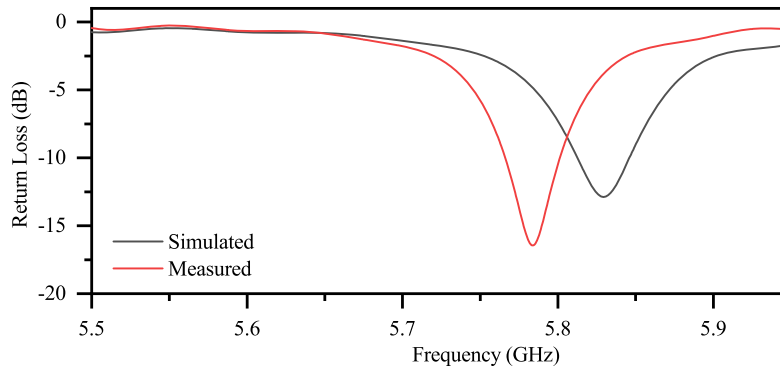


Figure 7. Simulated and measured reflection coefficients of antenna fed at port 1 when port 2 is terminated.

amount of power over the microstrip feed length due to signal fade along the feeder. This phenomenon is explained by referring to the simulated power magnitude on the microstrip line, as depicted in Figure 6.

The antenna resonance bandwidth is considered whenever the reflection coefficient is below 10 dB. It is depicted in Figures 7 and 11. The simulated and measured reflection coefficients are in good agreement. The simulated and measured input impedances plotted on Smith charts are depicted in Figures 8 and 12 to confirm the CP polarization. The measured and simulated co-polarized and cross-polarized patterns in the xz plane for the antenna fed at one port with the other terminated are depicted in Figures 8 and 12. Finally, the 3-dB axial ratios for simulation and measurement are depicted on Figures 10 and 14.

5.1. RHCP Results

The simulation and measurement results for the input return loss are given in Figure 7. The minimal measured return loss takes place at 5.78 GHz at -16.45 dB with an impedance of $48.72 + j6.36 \Omega$ and a bandwidth of 36 MHz from 5.766 GHz to 5.802 GHz. The minimal simulated return loss occurs at 5.82 GHz at -12.87 dB and an impedance of $47.21 + j7.73 \Omega$ with a bandwidth of 40 MHz ranging from 5.812 GHz to 5.846 GHz. The agreement between the simulated and measured results was fairly good. The Smith chart shown in Figure 8 represents the impedance matching as well as confirms the polarization type. As can be seen from the figure, the CP can be noticed as two orthogonal modes were excited. The chart shows that the antenna is CP as there is a sharp fall and immediate rise close to the operating frequency.

Figure 9 depicts the measured and simulated co-polarized and cross-polarized patterns in the xz -

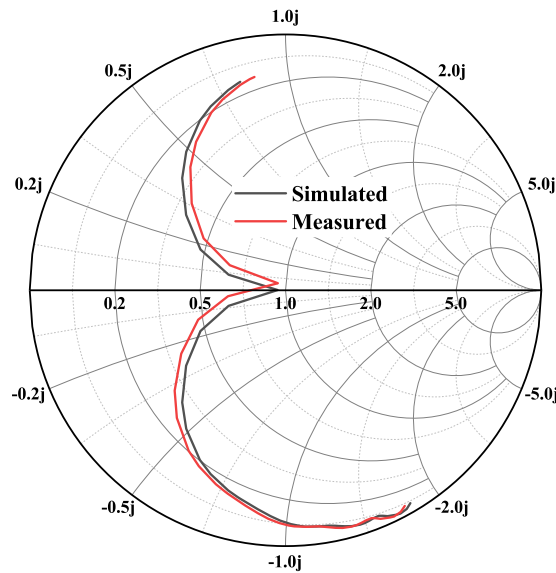


Figure 8. Input impedances on Smith chart sweep 5.5 GHz to 6 GHz.

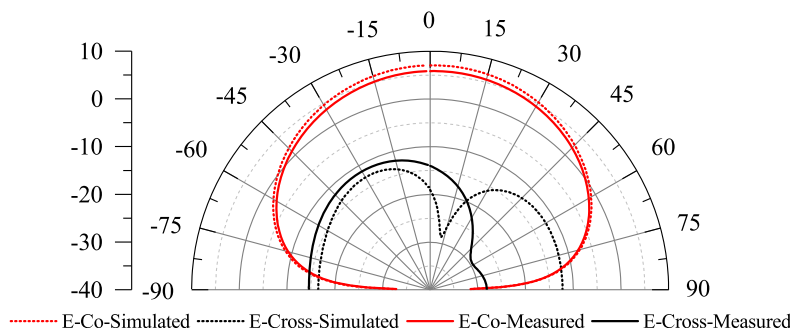


Figure 9. Simulated and measured 5.8-GHz radiation patterns in xz plane of antenna fed at port 1 when port 2 is terminated.

plane at 5.8 GHz. The cross-polarization is 19 dB lower than the co-polarization, which is a characteristic of RHCP radiation. The simulation results show good agreement with the measured radiation patterns. Good consistency between the simulation and measurement is attained.

Figure 10 demonstrates the axial ratio (AR) of the antenna. The axial ratio is found by measuring the fields in the vertical and horizontal planes. The simulated 3-dB AR bandwidth of the proposed antenna is from 5.79 to 5.86 GHz. The measured 3-dB AR bandwidth of the proposed antenna is from 5.77 to 5.86 GHz. A good agreement between the measured and simulated results can also be observed.

5.2. LHCP Results

The simulation and measurement results for the input return loss are given in Figure 11. The minimal measured input return loss is 5.76 GHz of -12.32 dB with an impedance of $49.23 + j1.53 \Omega$ and a bandwidth of 20 MHz from 5.754 GHz to 5.774 GHz. The minimal simulated return loss occurs at 5.79 GHz at -12 dB and an impedance of $49.75 + 2.13 \Omega$ with a bandwidth of 18 MHz ranging from 5.788 GHz to 5.806 GHz. Figure 12 depicts the simulated and measured Smith charts. The inflection point on the impedance curves indicates that two modes are formed yielding a CP radiation. Furthermore, it can be noticed that the axial ratio is minimal at the center frequency.

Figure 13 depicts the measured and simulated co-polarized and cross-polarized patterns in the xz plane at 5.8 GHz. The cross-polarization is 14 dB higher than the co-polarization, which is a

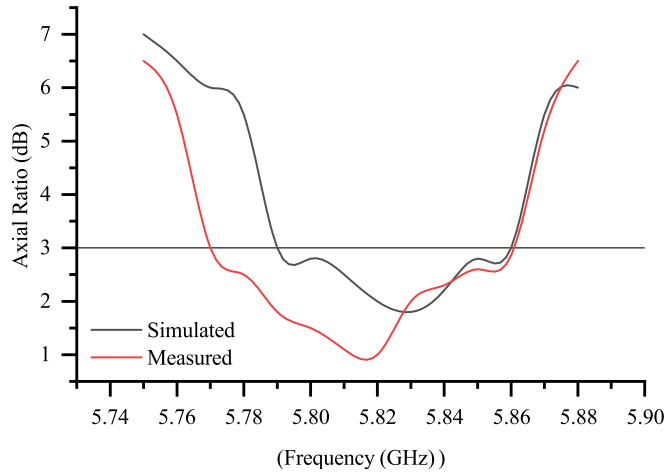


Figure 10. The simulated and measured 3-dB axial ratio.

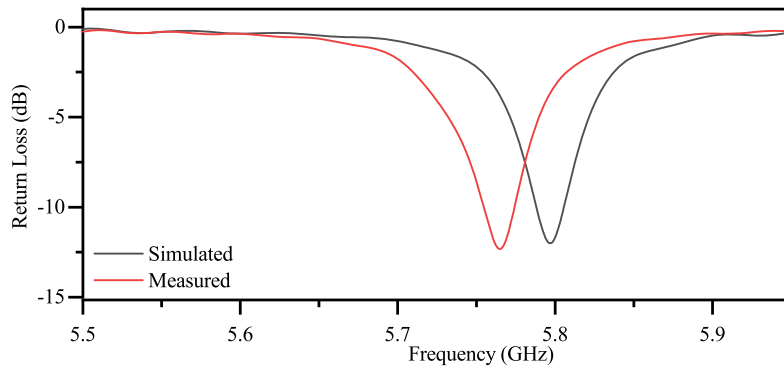


Figure 11. Simulated and measured reflection coefficients of antenna fed at port 2 when port 1 is terminated.

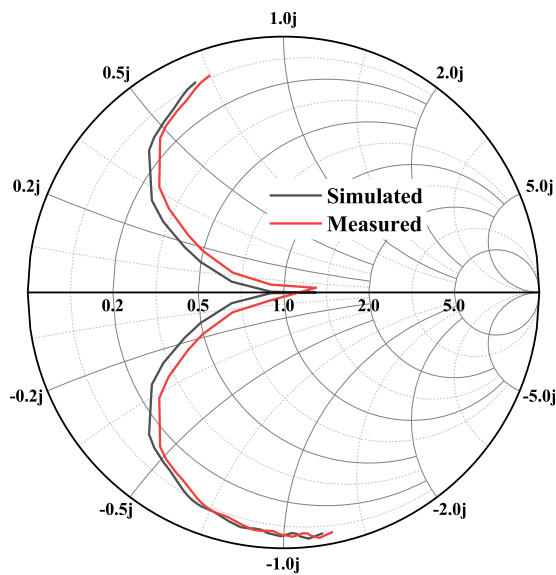


Figure 12. Input impedances on Smith chart sweep 5.5 GHz to 6 GHz.

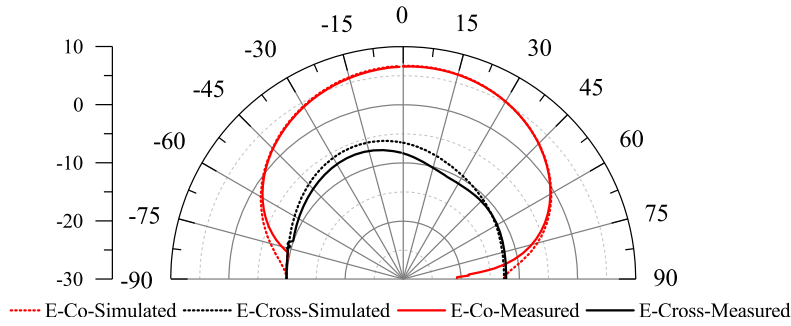


Figure 13. Simulated and measured 5.8-GHz radiation patterns in xz plane of antenna fed at port 2 when port 1 is terminated.

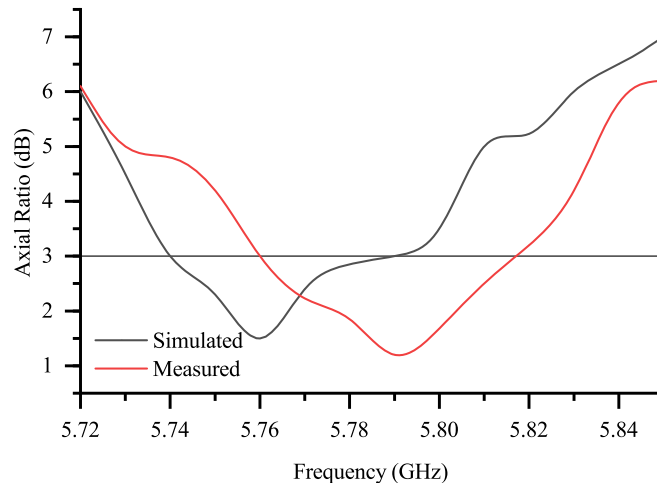


Figure 14. The simulated and measured 3-dB axial ratio.

characteristic of LHCP radiation. The measured radiation pattern matches well with the simulated results.

Figure 14 demonstrates the AR of the antenna. The AR is found by measuring the fields in the vertical and horizontal planes. The simulated 3-dB AR bandwidth of the proposed antenna is from 5.74 to 5.79 GHz. The measured 3-dB AR bandwidth of the proposed antenna is from 5.76 to 5.81 GHz. The agreement between simulation and measurement is obtained.

Table 3. A comparison between proposed QLR array with other dual polarized concentric ring microstrip arrays reported in the literature.

Reference	Size [mm ²]	Number of array elements
Chaudhuri et al. (2019) [27]	165 × 165	10
Chen et al. (2017) [28]	63 × 63	7
Min et al. (2009) [29]	Feeder placed on radius of 31 mm [exact size is not mentioned]	6
Yang et al. (2018) [2]	Feeder placed on radius of 20 mm [exact size is not mentioned]	8
Proposed work	40 × 40	7

6. CONCLUSION

A dual circularly polarized concentric ring series-fed quasi-lumped antenna array was proposed. By feeding the antenna ports simultaneously, LHCP and RHCP can be obtained accordingly. The antenna was fabricated and experimentally validated. The main attraction of the proposed antenna design is its miniaturized real state size. The agreement between the simulated and experimental results authenticated the design. A comparison was made between various reported differential ring microstrip-fed dual-CP arrays and the array reported in this communication which is presented in Table 3. The comparison showed a significant size reduction compared with those documented in the literature.

ACKNOWLEDGMENT

The authors thank the anonymous reviewers for their constructive comments.

REFERENCES

1. Masa-Campos, J. L. and F. Gonzalez-Fernandez, "Dual linear/circular polarized planar antenna with low profile double-layer polarizer of 45° tilted metallic strips for WiMAX applications," *Progress In Electromagnetics Research*, Vol. 98, 221–231, 2009.
2. Yang, Y., J. Guo, Y. Cia, and G. Zhou, "The design of dual circularly polarized series-fed array," *IEEE Transactions on Antennas and Propagation*, Vol. 67, No. 1, 574–579, 2019.
3. Wu, G.-L., W. Mu, G. Zhao, and Y.-C. Jiao, "A novel design of dual circularly polarized antenna fed by L-strip," *Progress In Electromagnetics Research*, Vol. 79, 39–46, 2008.
4. Liu, H., Y. Liu, and S. Gong, "Design of a compact dual-polarised slot antenna with enhanced gain," *IET Microwaves, Antennas & Propagation*, Vol. 11, No. 6, 892–897, 2017.
5. Jin, H., K. Chin, W. Che, C. Chang, H. Li, and Q. Xue, "Differential-fed patch antenna arrays with low cross polarization and wide bandwidths," *IEEE Antennas and Wireless Propagation Letters*, Vol. 13, 1069–1072, 2014.
6. Li, B., Y. Yin, W. Hu, Y. Ding, and Y. Zhao, "Wideband dual-polarized patch antenna with low cross polarization and high isolation," *IEEE Antennas and Wireless Propagation Letters*, Vol. 11, 427–430, 2012.
7. Zhang, Y. P. and J. J. Wang, "Theory and analysis of differentially-driven microstrip antennas," *IEEE Transactions on Antennas and Propagation*, Vol. 54, No. 4, 1092–1099, 2006.
8. Amiri, N. and K. Forooghi, "Dual-band and dual-polarized microstrip array antenna for GSM900/DCS1800 MHz base stations," *IEEE Antennas and Propagation Society International Symposium*, 4439–4442, NM, 2006.
9. Karimkashi, S. and G. Zhang, "A dual-polarized series-fed microstrip antenna array with very high polarization purity for weather measurements," *IEEE Transactions on Antennas and Propagation*, Vol. 61, No. 10, 5315–5319, 2013.
10. Vallecchi, A. and B. Gentili, "Design of dual-polarized series-fed microstrip arrays with low losses and high polarization purity," *IEEE Transactions on Antennas and Propagation*, Vol. 53, No. 5, 1791–1798, 2005.
11. Chen, S. J., C. Fumeaux, Y. Monnai, and W. Withayachumnankul, "Dual circularly polarized series-fed microstrip patch array with coplanar proximity coupling," *IEEE Antennas and Wireless Propagation Letters*, Vol. 16, 1500–1503, 2017.
12. Shen, Y., S. Zhou, Y. Huang, and T. Chio, "A compact dual circularly polarized microstrip patch array with interlaced sequentially rotated feed," *IEEE Transactions on Antennas and Propagation*, Vol. 64, No. 11, 4933–4939, 2016.
13. Zhang, G., Q. Lin, L. Nie, J. Yu, and Y. Fan, "Wideband dual-polarization patch antenna array with parallel strip line balun feeding," *IEEE Antennas and Wireless Propagation Letters*, Vol. 15, 1499–1501, 2016.

14. Cui, Y., X. Gao, and R. Li, "A broadband differentially fed dual-polarized planar antenna," *IEEE Transactions on Antennas and Propagation*, Vol. 65, No. 6, 3231–3234, 2017.
15. Sun, K., D. Yang, Y. Chen, and S. Liu, "A broadband commonly fed dual-polarized antenna," *IEEE Antennas and Wireless Propagation Letters*, Vol. 17, No. 5, 747–750, 2018.
16. Tang, Z., J. Liu, and Y. Yin, "Enhanced cross-polarization discrimination of wideband differentially fed dual-polarized antenna via a shorting loop," *IEEE Antennas and Wireless Propagation Letters*, Vol. 17, No. 8, 1454–1458, 2018.
17. White, C. R. and G. M. Rebeiz, "A differential dual-polarized cavity-backed microstrip patch antenna with independent frequency tuning," *IEEE Transactions on Antennas and Propagation*, Vol. 58, No. 11, 3490–3498, 2010.
18. Zhang, F., F. Zhu, and S. Gau, "Differential-fed ultra-wideband slot-loaded patch antenna with dual orthogonal polarisation," *Electronics Letters*, Vol. 49, No. 25, 1591–1593, 2013.
19. Xue, Q., S. Liao, and J. Xu, "A differentially-driven dual-polarized magneto-electric dipole antenna," *IEEE Transactions on Antennas and Propagation*, Vol. 61, No. 1, 425–430, 2013.
20. Xue, Q., S. Liao, and J. Xu, "A differentially-driven dual-polarized magneto-electric dipole antenna," *IEEE Transactions on Antennas and Propagation*, Vol. 61, No. 1, 425–430, 2013.
21. Luo, Y. and Q. Chu, "Oriental crown-shaped differentially fed dual-polarized multidipole antenna," *IEEE Transactions on Antennas and Propagation*, Vol. 63, No. 11, 4678–4685, 2015.
22. Luo, Q., S. Gao, M. Sobhy, J. Sumantyo, J. Li, G. Wei, J. Xu, and C. Wu, "Dual circularly polarized equilateral triangular patch array," *IEEE Transactions on Antennas and Propagation*, Vol. 64, No. 6, 2255–2262, 2016.
23. Bahl, I. J., *Lumped Elements for RF and Microwave Circuits*, Artech House, Boston, 2003.
24. Huang, F., B. Avenhaus, and M. Lancaster, "Lumped-element switchable superconducting filters," *IEE Proceedings — Microwaves, Antennas and Propagation*, Vol. 146, No. 3, 229–233, 1999.
25. Bogatin, E., "Design rules for microstrip capacitance," *IEEE Transactions on Components, Hybrids, and Manufacturing Technology*, Vol. 11, No. 3, 253–259, 1988.
26. Su, H. T., M. J. Lancaster, F. Huang, and F. Wellhofer, "Electrically tunable superconducting quasilumped element resonator using thin-film ferroelectrics," *Microwave and Optical Technology Letters*, Vol. 24, 155–158, 2000.
27. Chaudhuri, S., R. S. Kshetrimayum, R. K. Sonkar, and M. Mishra, "Dual circularly polarised travelling wave slot antenna array," *Electronics Letters*, Vol. 55, No. 20, 1071–1073, 2019.
28. Chen, S. G., C. Fumeaux, M. Monnai, and W. Withayachumnankul, "Dual circularly polarized series-fed microstrip patch array with coplanar proximity coupling," *IEEE Antennas and Wireless Propagation Letters*, Vol. 16, No. 10, 1500–1503, 2017.
29. Min, C. and C. E. Free, "Analysis of traveling-wave-fed patch arrays," *IEEE Transactions on Antennas and Propagation*, Vol. 57, No. 3, 664–670, 2009.

Erratum to “Design of Compact Dual Circularly Polarized Concentric Ring Series-Fed Quasi-Lumped Antenna Array”

by Yazeed Qasaymeh, Abdullah Almuhasien, and Khaled Issa
in *Progress in Electromagnetic Research C*, Vol. 103, 111–121, 2020

Yazeed Qasaymeh^{1, *}, Abdullah Almuhasien¹, and Khaled Issa²

The first and second authors' affiliation should be:

¹ Department of Electrical Engineering, College of Engineering, Majmaah University, Al-Majmaah 11952, Saudi Arabia

Received 24 November 2021, Added 26 November 2021

* Corresponding author: Yazeed Qasaymeh (y.qasaymeh@mu.edu.sa).

¹ Department of Electrical Engineering, College of Engineering, Majmaah University, Al-Majmaah 11952, Saudi Arabia. ² KACST-TIC in Radio Frequency and Photonics for the e-Society (RFTONICS), Electrical Engineering Department, King Saud University, Riyadh, Saudi Arabia.